J. Phys.: Condens. Matter **12** (2000) 7569–7582. Printed in the UK PII: S0953-8984(00)13641-0

One-phonon relaxation of localized electronic states in anharmonic nanoparticles

Vadim A Markel† and Michael R Geller

Department of Physics and Astronomy, University of Georgia, Athens, GA 30602-2451, USA

E-mail: vmarkel@ee.wustl.edu

Received 2 May 2000

Abstract. There is currently great interest in the dynamics of electrons and phonons in low-dimensional systems, where the effects of quantum confinement cause a dramatic difference in their behaviour as compared with bulk systems. In this paper we consider a localized electronic impurity state (an electronic two-level system) linearly coupled to the vibrational modes of an isolated nanometre-scale insulating crystal, and study the phonon emission rate at frequencies less than that of the lowest internal vibrational mode, i.e., in the acoustic 'gap'. We show that, at finite temperature, electronic energy relaxation below the acoustic gap can occur as a result of anharmonic broadening of vibrational modes, and we calculate the frequency and temperature dependence of the relaxation provided by this mechanism.

1. Introduction

It is well known that the vibrational density of states (DOS) forms a continuous band in bulk solids, and at low energies is well described by the Debye law [1]. However, in small crystals the finite size leads to a discretization of the phonon spectrum. This is strongly manifested at low frequencies where the separation between modes may become larger than their width, and no modes exist below the lowest vibrational frequency. We shall refer to the frequency $\omega_{\min}$ of the lowest vibrational mode as the acoustic 'gap', even though it is not a gap in the strict sense. The discrete DOS is expected to change dramatically any physical processes involving low-frequency phonons, such as one-phonon energy relaxation and dephasing of closely spaced electronic states, two-phonon Raman scattering, and anharmonic interactions.

Although electron–phonon processes have been extensively studied for bulk systems [2,3], much less is known about nanocrystalline materials. Most of the work on the optical properties of non-metallic nanocrystals has been on semiconductor nanocrystals [4, 5] and semiconductor quantum dots [6–8], which are especially interesting for device applications. The principal concern for device applications (quantum dot lasers, for example) is the influence of phonon confinement on electron and hole intraband relaxation [9], which, in a bulk semiconductor, is usually dominated by LO phonon emission. In contrast, our focus is on low-energy (a few cm^{-1}) acoustic phonon emission by localized impurity states in large-band-gap *doped* semiconductors and insulators, where striking phonon-confinement effects have been observed [10–12]. Measurements of this type are a direct and sensitive probe of the nanocrystal's vibrational DOS inside the acoustic gap.

† Currently at: Department of Electrical Engineering, Washington University, Campus Box 1127, St Louis, MO 63130-4899, USA.

0953-8984/00/347569+14$30.00 © 2000 IOP Publishing Ltd

Recently, Yang and co-workers measured the decay rates of Eu^{3+} impurity states separated by 3 cm^{-1} and 7 cm^{-1} in Y_2O_3 nanoparticles with sizes varying from 7 to 23 nm [11, 12]. Nanoparticles in this size range are unable to support phonons with the energy of 3 cm^{-1}. (The acoustic gap in a nanoparticle of size d can be estimated as $\omega_{min} \approx c/d$, where c is a characteristic sound speed. For Y_2O_3, $c \approx 7 \times 10^5$ cm s^{-1}, which gives 5 $cm^{-1} < \omega_{min} <$ 16 cm^{-1} for 23 nm $> d >$ 7 nm.) The lack of phonons which are resonant with the electronic transition prohibits direct one-phonon processes, and the absence of lower-frequency phonons prevents multi-phonon emission. Indeed, the rate of transitions between the components of the 3 cm^{-1} pair was found to be approximately 300 times smaller than the corresponding rate for a bulk sample (in which the direct one-phonon process is allowed) but not zero, with essentially no temperature dependence in the range of 1.5–10 K. Since this relaxation is still much faster than the radiative decay rate, its origin needs to be understood.

One of the possible mechanisms for such transitions is the two-phonon Raman process in which a thermal phonon is absorbed by the excited-state electron and a phonon of higher frequency is emitted. The rate of transitions due to two-phonon Raman scattering in a Debye system scales with temperature as T^7 [2]. However, the two-phonon Raman rate for transitions between the same levels in a bulk system (at the same temperature) is much smaller than was observed, and is expected to be further suppressed in a nanocrystal.

Another important class of mechanisms comprises those due to the interaction of a nanoparticle with its surroundings. From the experiments of references [11] and [12], nanoparticles are known to form self-supporting clusters. Such clusters can have collective vibrational modes with frequencies low enough to allow direct one-phonon relaxation. Another possible mechanism of electronic relaxation is interaction with molecules adsorbed on a nanoparticle's surface when the impurity electron wave function has significant tails extending to the nanoparticle boundary (this can happen if the impurity is located close to the surface), or if the interaction with the molecule is long ranged (for example, electric dipole interaction). Finally, the vibrational modes of a nanoparticle may be broadened by direct mechanical interaction with a cluster, substrate, or support matrix if that interaction is strong enough, and electronic relaxation can occur via the tails of these broadened modes.

In this paper we study the one-phonon electronic relaxation for transition energies below the acoustic gap that becomes possible because of an uncertainty in the phonon energy originating from intrinsic phonon relaxation. Intrinsic relaxation of phonons, in turn, can have many origins. One of them, which is always present, is phonon–phonon interaction due to anharmonicity of the crystal. The lowest-order (cubic) anharmonicity leads to second-order non-linear processes such as second-harmonic generation or combination scattering. In the case of the second-harmonic generation, a phonon of a given frequency ω can decay into two phonons of frequencies ω_1 and ω_2 with $\omega_1 + \omega_2 = \omega$. The broadening of phonon energies makes a direct one-phonon process possible even if there are no free phonons with frequencies at the transition energy.

We will make two basic assumptions concerning the nanoparticles.

First, since the exact shape and structure of the nanoparticles in question are not known, and our aim is a general consideration of possible relaxation mechanisms rather than a precise fitting of experimental results, we adopt a simplified model for the nanoparticle DOS. Namely, we assume that the DOS $\rho(\omega)$ is Debye-like for $\omega_{min} < \omega < \omega_D$ (ω_D is the bulk Debye frequency) and zero below ω_{min}:

$$\rho(\omega) = \sum_{n=1}^{N} \delta(\omega - \omega_n) = \begin{cases} \dfrac{3N\omega^2}{(\omega_D^3 - \omega_{min}^3)} & \text{if } \omega_{min} < \omega < \omega_D \\ 0 & \text{otherwise} \end{cases} \tag{1}$$

where the ω_n are phonon eigenfrequencies and N is the total number of vibrational modes†.

Second, we consider nanoparticles to be isolated. By doing this, we exclude from consideration the *extrinsic* relaxation mechanisms mentioned above. Violation of this condition will clearly lead to changes in the model DOS (1).

The paper is organized as follows. In section 2 we derive perturbatively the one-phonon relaxation rate from the linear strain electron–phonon interaction for a solid with a general phonon DOS. In the case of free (undamped) phonons, this expression yields a zero transition rate for frequencies in the acoustic gap. However, if phonon damping is included, the rate becomes non-zero. In sections 3 and 4 we calculate the electron relaxation rate in the case of damped phonons. In section 3 the phonon spectral functions are considered to be Lorentzians, the width of each Lorentzian being the relaxation rate of the corresponding phonon. It is shown that this naive treatment leads to blatant contradictions with experiment. In section 4 we explain this contradiction by showing that it is necessary to take into account the frequency dependence of the phonon self-energy. In section 5 we derive the frequency-dependent self-energy for the case where the phonon relaxation results from cubic lattice anharmonicity. Section 6 contains a summary of our results.

2. Linear electron–phonon interaction

We consider a model of a two-level system described by Fermi creation and annihilation operators $c_\alpha^\dagger$, c_α ($\alpha = 0, 1$) coupled linearly to (scalar) phonons with Bose creation and annihilation operators $a_n^\dagger$ and a_n, corresponding to the nth mode with frequency ω_n. The Hamiltonian of this system is (in a system of units where $\hbar = 1$)‡

$$H = H_0 + \delta H \tag{2}$$

$$H_0 = \sum_\alpha (\epsilon_\alpha - \mu) c_\alpha^\dagger c_\alpha + \sum_n \omega_n a_n^\dagger a_n \tag{3}$$

$$\delta H = \sum_n g_n (a_n c_0 c_1^\dagger + a_n^\dagger c_1 c_0^\dagger). \tag{4}$$

Here H_0 is the unperturbed Hamiltonian of a two-level system with energy levels ϵ_0 and ϵ_1, and that of the free-phonon system; μ is the chemical potential. δH is the electron–phonon interaction term with the g_ns being the (real) coefficients in the expansion of the displacement field in terms of a_n and $a_n^\dagger$, multiplied by a factor that characterizes the strength of the electron–phonon interaction. These constants are chosen to have the dimensionality of energy, and depend on ω_n and the total number of eigenmodes N (or the sample volume V) as $g_n \propto \sqrt{\omega_n/N} \propto \sqrt{\omega_n/V}$. The functional dependence of the g_ns on ω_n and N follows from the general properties of the expansion of the quantized phonon displacement field and is independent of the electron–phonon interaction [13]. The Hamiltonian (2) is standard in condensed matter theory [13] and quantum optics [14]. δH is referred to as the linear strain interaction because it is linear in the phonon field. It can be also interpreted as an electron–photon interaction Hamiltonian in the dipole approximation.

The standard approach used to determine the transition rate is based on a calculation of the retarded Green's function for the electron in the state $\alpha = 1$, defined as

$$G_{\mathrm{ret}}(t) = -\mathrm{i}\Theta(t)\langle\{c_1(t), c_1^\dagger(0)\}\rangle \tag{5}$$

† Note that we do not consider the optical branch of vibrational modes. The latter can be described by a delta-function-type DOS centred near ω_{D}, and can be easily accounted for in all calculations, without influencing the results qualitatively.

‡ The electrons are taken to be spinless for simplicity.

where $\langle A\rangle \equiv \mathrm{Tr}(\mathrm{e}^{-\beta H}A)/\mathrm{Tr}(\mathrm{e}^{-\beta \mathrm{H}})$, $\Theta(t)$ is the step function, and the operators are in the Heisenberg representation. The Fourier transform of (5) is given by

$$G_{\mathrm{ret}}(\omega) \equiv \int_{-\infty}^{\infty} G_{\mathrm{ret}}(t)\mathrm{e}^{\mathrm{i}\omega t}\,\mathrm{d}t = \frac{1}{\omega - \xi_1 - \Sigma_{\mathrm{ret}}(\omega)} \tag{6}$$

where $\xi_\alpha \equiv \epsilon_\alpha - \mu$ and $\Sigma_{\mathrm{ret}}(\omega)$ is the retarded self-energy for the state $\alpha = 1$. The relaxation rate (in the conventional quasiparticle-pole approximation) is calculated by evaluating the imaginary part of the self-energy at the frequency corresponding to the pole of the unperturbed Green's function,

$$\tau_1^{-1} = -2\,\mathrm{Im}\,\Sigma_{\mathrm{ret}}(\omega = \xi_1). \tag{7}$$

The self-energy can be evaluated using conventional imaginary-time perturbation theory [13]. In the leading (second) order, the self-energy diagram is

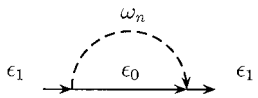

After analytic continuation, this self-energy may be written in terms of the non-interacting retarded phonon propagator†:

$$D_{\mathrm{ret}}^{(0)}(n,t) \equiv -\mathrm{i}\Theta(t)\langle[a_n(t), a_n^{\dagger}(0)]\rangle_0 = -\mathrm{i}\Theta(t)\mathrm{e}^{-\mathrm{i}\omega_n t} \tag{8}$$

$$D_{\mathrm{ret}}^{(0)}(n,\omega) \equiv \int_{-\infty}^{\infty} D_{\mathrm{ret}}^{(0)}(n,t)\mathrm{e}^{\mathrm{i}\omega t}\,\mathrm{d}t = \frac{1}{\omega - \omega_n + \mathrm{i}0} \tag{9}$$

where $\langle A\rangle_0 \equiv \mathrm{Tr}(\mathrm{e}^{-\beta H_0}A)/\mathrm{Tr}(\mathrm{e}^{-\beta \mathrm{H}_0})$ and O is an infinitesimally small positive number introduced for regularization of the Fourier transformation. One can easily obtain for the electron self-energy

$$\Sigma_{\mathrm{ret}}(\omega) = \sum_n g_n^2\,[n_{\mathrm{B}}(\omega_n) + n_{\mathrm{F}}(-\xi_0)]\,D_{\mathrm{ret}}^{(0)}(n, \omega - \xi_0) \tag{10}$$

where $n_{\mathrm{B}}(z) = 1/[\exp(z/T) - 1]$ and $n_{\mathrm{F}}(z) = 1/[\exp(z/T) + 1]$ are the Bose and Fermi distribution functions, respectively, and T is the temperature (in units such that Boltzmann's constant is one). In order to consider electronic relaxation in the situation where the final state is not occupied in thermal equilibrium (i.e., it is available for the transition), we set the chemical potential μ so that $n_{\mathrm{F}}(\xi_0) = 0$.

Next, we introduce a coupling-constant-weighted DOS

$$\Gamma(\omega) \equiv \sum_n g_n^2 \delta(\omega - \omega_n). \tag{11}$$

It is evident from equations (9) and (10) that it is the weighted DOS rather than the thermodynamic DOS (1) that governs the frequency dependence of Σ_{ret}. The frequency dependence of $\Gamma(\omega)$ for our nanoparticle model follows from (1) and the fact that $g_n \propto \sqrt{\omega_n/N}$. Evidently, $\Gamma(\omega)$ is equal to zero in the gap and proportional to ω^3 for $\omega_{\min} < \omega < \omega_{\mathrm{D}}$:

$$\Gamma(\omega) = \begin{cases} 4\kappa\omega_{\mathrm{D}}^2\omega^3/(\omega_{\mathrm{D}}^4 - \omega_{\min}^4) & \text{if } \omega_{\min} < \omega < \omega_{\mathrm{D}} \\ 0 & \text{otherwise} \end{cases} \tag{12}$$

where

$$\kappa \equiv \left(\sum_n g_n^2\right)\Big/\omega_{\mathrm{D}}^2. \tag{13}$$

† This definition differs from the definition adopted in most standard texts (e.g., see [13]), where phonon propagators have no time direction.

The dimensionless parameter κ characterizes the electron–phonon interaction strength. It does not depend on the total number of modes or the sample volume, as long as $\omega_{\min} \ll \omega_{\mathrm{D}}$, because $g_n^2 \propto 1/N$ and the total number of terms in the summation (13) is N.

Substituting unity for $n_{\mathrm{F}}(-\xi_0)$, and using definitions (9) and (11), we obtain

$$\Sigma_{\mathrm{ret}}(\omega) = \int \Gamma(\omega') \frac{n_{\mathrm{B}}(\omega') + 1}{\omega - \xi_0 - \omega' + \mathrm{i}0} \, \mathrm{d}\omega'. \tag{14}$$

Using

$$\mathrm{Im}\left[\frac{1}{\omega - \xi_0 - \omega' + \mathrm{i}0}\right] = -\pi\delta(\omega - \xi_0 - \omega') \tag{15}$$

we arrive at

$$\mathrm{Im}\,\Sigma_{\mathrm{ret}}(\omega) = -\pi\Gamma(\omega - \xi_0)[n_{\mathrm{B}}(\omega - \xi_0) + 1]. \tag{16}$$

As discussed above, in the quasiparticle-pole approximation the self-energy is evaluated at $\omega = \xi_1$, which yields the relaxation rate

$$\tau_1^{-1} = 2\pi\Gamma(\Delta\epsilon)[n_{\mathrm{B}}(\Delta\epsilon) + 1] \tag{17}$$

where we have introduced the electronic energy level spacing

$$\Delta\epsilon \equiv \epsilon_1 - \epsilon_0. \tag{18}$$

The brief discussion outlined above summarizes the standard approach to electronic relaxation of a two-level system coupled to phonons. Formula (17) is the Fermi golden rule result for the rate of transitions between two electronic levels. It is given by a sum of two terms: the first one, proportional to $n_{\mathrm{B}}(\Delta\epsilon)$, is the stimulated transition rate which is proportional to the number of thermal phonons with energies $\Delta\epsilon$. The second term describes spontaneous relaxation and can occur at zero temperature.

It is clear that the transition rate, according to (17), is always zero when $\Delta\epsilon < \omega_{\min}$. In the following sections we consider the damping of phonons, which leads to replacement of the delta functions in (15) by functions which have tails extending into the gap, as a possible explanation of the experimentally observed relaxation.

3. Lorentzian broadening of phonons

As a first attempt at explaining the observed transition rate for $\Delta\epsilon < \omega_{\min}$, we consider the damping of phonons. Physically, this means that there is an uncertainty in the phonon energy ω_n. The reciprocal of this uncertainty is the phonon relaxation time which is experimentally measurable. The relaxation of phonons can occur due to a variety of physical reasons, such as absorption by the environment at the boundary of a nanoparticle, anharmonicity, and inelastic scattering by impurities and lattice defects.

We start by observing that in the case of phonon damping, the free-phonon propagators $D_{\mathrm{ret}}^{(0)}(n, \omega)$ appearing in (10) should be replaced by the (diagonal-in-n) interacting propagators $D_{\mathrm{ret}}(n, \omega)$, defined analogously to (8) and (9), but with H_0 replaced by the full interacting Hamiltonian, including the terms that are responsible for phonon damping. This follows directly from the perturbation expansion where the electron–phonon interaction is treated to second order, but other interactions (such as the phonon–phonon interaction) are treated to all orders. The excited-state electron self-energy becomes

$$\Sigma_{\mathrm{ret}}(\omega) = \sum_n g_n^2[1 + \tilde{n}_{\mathrm{B}}(\omega_n)]D_{\mathrm{ret}}(n, \omega - \xi_0). \tag{19}$$

The tilde sign over n_{B} is used to indicate that the occupation numbers have to be evaluated at renormalized frequencies, as discussed below. In the simplest case, we can introduce the phonon damping by replacing the infinitesimal imaginary term in (9) by a finite constant η:

$$D_{\mathrm{ret}}(n,\omega)=\frac{1}{\omega-\omega_n+\mathrm{i}\eta}. \tag{20}$$

In reality, η depends on the quantum number n. However, to demonstrate the shortcomings of the Lorentzian line-shape assumption it is sufficient to take η to be n-independent; we shall show below that including the correct n-dependence (for the case of anharmonic broadening) makes the agreement with experiment even worse.

Initially we will assume that η is independent of frequency. In this approximation, the phonon relaxation time is given by η^{-1}. This leads to

$$\tau_1^{-1}=\int\Gamma(\omega)\frac{\eta[1+\mathrm{Re}\,n_{\mathrm{B}}(\omega-\mathrm{i}\eta)]-(\Delta\epsilon-\omega)\,\mathrm{Im}\,n_{\mathrm{B}}(\omega-\mathrm{i}\eta)}{(\Delta\epsilon-\omega)^2+\eta^2}\,\mathrm{d}\omega. \tag{21}$$

Now the relaxation rate is finite when $\Delta\epsilon<\omega_{\min}$ due to the tails of the Lorentzian factors in the integrand of (21).

First, we consider the low-temperature case, when $T\ll\omega_{\min}$. The Bose occupation factors in (21) can then be neglected. We use expression (12) for $\Gamma(\omega)$ to obtain

$$\tau_1^{-1}(\Delta\epsilon)=\frac{4\kappa\omega_{\mathrm{D}}^2\eta}{\omega_{\mathrm{D}}^4-\omega_{\min}^4}\int_{\omega_{\min}}^{\omega_{\mathrm{D}}}\frac{\omega^3\,\mathrm{d}\omega}{(\omega-\Delta\epsilon)^2+\eta^2}. \tag{22}$$

This integral can be easily evaluated and yields

$$\begin{aligned}\tau_1^{-1}(\Delta\epsilon)=\frac{4\kappa\omega_{\mathrm{D}}^2\eta}{\omega_{\mathrm{D}}^4-\omega_{\min}^4}\Bigg[&\left(\frac{\Delta\epsilon^3}{\eta}-3\,\Delta\epsilon\,\eta\right)\left(\arctan\frac{\omega_{\mathrm{D}}-\Delta\epsilon}{\eta}+\arctan\frac{\Delta\epsilon-\omega_{\min}}{\eta}\right)\\&+\left(\frac{3\,\Delta\epsilon^2}{2}-\frac{\eta^2}{2}\right)\ln\frac{(\omega_{\mathrm{D}}-\Delta\epsilon)^2+\eta^2}{(\omega_{\min}-\Delta\epsilon)^2+\eta^2}+\frac{\omega_{\mathrm{D}}^2-\omega_{\min}^2}{2}+2\,\Delta\epsilon(\omega_{\mathrm{D}}-\omega_{\min})\Bigg].\end{aligned} \tag{23}$$

An important feature of the above formula is that the transition rate in the gap is dominated by the input of *high-frequency* modes and is insensitive to the local structure of $\Gamma(\omega)$ near $\omega=\omega_m$. Including the n-dependence of η would only enhance this effect. This feature can be easily seen by evaluating the integral (22) with $\Delta\epsilon=\eta=0$, in which case it becomes proportional to $\omega_{\mathrm{D}}^2-\omega_{\min}^2\approx\omega_{\mathrm{D}}^2$. It can be also verified by observing that

$$\begin{aligned}\lim_{\eta\to0}&\left(\arctan\frac{\omega_{\mathrm{D}}-\Delta\epsilon}{\eta}+\arctan\frac{\Delta\epsilon-\omega_{\min}}{\eta}\right)\\&=\begin{cases}\pi & \text{if } \Delta\epsilon>\omega_{\min}\\ \dfrac{\eta(\omega_{\mathrm{D}}-\omega_{\min})}{(\omega_{\min}-\Delta\epsilon)(\omega_{\mathrm{D}}-\Delta\epsilon)} & \text{if } \Delta\epsilon<\omega_{\min}.\end{cases}\end{aligned} \tag{24}$$

Therefore, the dominant term in the square brackets in (23) becomes $\omega_{\mathrm{D}}^2/2$ when $\Delta\epsilon<\omega_{\min}$ and $\eta\ll|\omega_{\mathrm{D}}-\Delta\epsilon|,|\omega_{\min}-\Delta\epsilon|$. For a small η and $\omega_{\mathrm{D}}\gg\omega_{\min}$, the transition rate can be approximately written as

$$\tau_1^{-1}\approx\frac{4\kappa}{\omega_{\mathrm{D}}^2}\left(\pi(\Delta\epsilon)^3\Theta(\Delta\epsilon-\omega_{\min})+\frac{\eta\omega_{\mathrm{D}}^2}{2}\right). \tag{25}$$

The first term in the above formula is proportional to $\Gamma(\Delta\epsilon)$ and, therefore, is equivalent to expression (17) obtained in the limit $\eta\to0$ by replacing Lorentzians in the integrand of (22) by delta functions. The second term is due to the finite value of η and becomes dominant when

$\Delta\epsilon\,\Theta(\Delta\epsilon - \omega_{\min}) < \epsilon_c$, where $\epsilon_c \equiv (\eta\omega_D^2/2\pi)^{1/3}$. In particular, for the Debye DOS without a gap (i.e., with $\omega_{\min} = 0$), the cubic dependence of τ_1^{-1} on $\Delta\epsilon$ crosses over to the constant value $\tau_1^{-1} = 2\kappa\eta$ at energies smaller than ϵ_c.

The behaviour of $\tau_1^{-1}(\Delta\epsilon, \eta)$ is illustrated in figure 1. In figure 1(a), we plot the dependence of τ_1^{-1} on $\Delta\epsilon$ for a constant value of $\eta = 0.1\ \mathrm{cm}^{-1}$. Two curves are shown: one for a DOS with a gap at $\omega_{\min} = 10\ \mathrm{cm}^{-1}$ and the other for the Debye DOS without a gap. The two curves are virtually indistinguishable. This is explained by the fact mentioned above that the dominant contribution at small $\Delta\epsilon$ is due to tails of the high-frequency modes. The

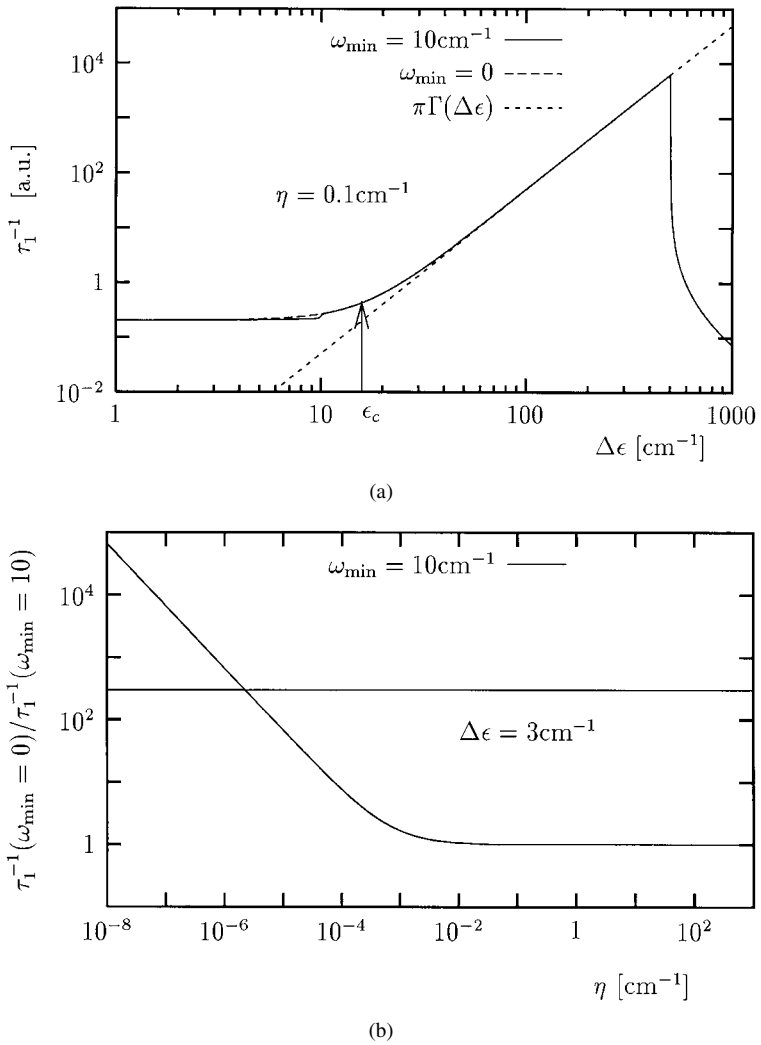

Figure 1. (a) Transition rate τ_1^{-1} as a function of $\Delta\epsilon$ for the DOS with a gap at $\omega_{\min} = 10\ \mathrm{cm}^{-1}$ and without a gap ($\omega_{\min} = 0$) compared to the result given by formula (17) at zero temperature. Here $\omega_D = 500\ \mathrm{cm}^{-1}$ and $\eta = 0.1\ \mathrm{cm}^{-1}$. The crossover value ϵ_c is indicated by a vertical arrow. (b) The ratio of the transition rate in a bulk material to that in a nanoparticle with a gap at $\omega_{\min} = 10\ \mathrm{cm}^{-1}$ for $\Delta\epsilon = 3\ \mathrm{cm}^{-1}$. The experimentally measured ratio of 300 [11, 12] is indicated by a horizontal line. The curves for other values of $\omega_{\min}$ such that $\omega_{\min} > 3\ \mathrm{cm}^{-1}$ are virtually indistinguishable from the curve shown in the figure.

crossover from cubic dependence on $\Delta\epsilon$ to a constant is seen for the Debye DOS at $\Delta\epsilon < \epsilon_c$. This clearly contradicts experiment (e.g., see [16]).

In figure 1(b), we plot the ratio of the transition rate in a bulk material ($\omega_{\min} = 0$) to that of a nanoparticle with a gap at $\omega_{\min} = 10\ \mathrm{cm}^{-1}$ for $\Delta\epsilon = 3\ \mathrm{cm}^{-1}$. These numerical values approximately correspond to the experimental situation [11, 12]. As can be seen from figure 1(b), the experimentally observable ratio of ∼300 is achieved for $\eta \approx 10^{-5}\ \mathrm{cm}^{-1}$. This is an extremely small value and is inconsistent with experimental results. Note that the curves for other values of $\omega_{\min}$ in the range $5\ \mathrm{cm}^{-1} < \omega_{\min} < 15\ \mathrm{cm}^{-1}$ are virtually indistinguishable from the one shown in figure 1(b).

Although we see that the model of damped phonons with a constant width η leads to serious contradictions, it does describe accurately one of the experimentally observed effects, namely, the absence of temperature dependence of the transition rate in the temperature range of 1.5–10 K. This is explained by the fact that the high-frequency modes that give the dominant input to the transition rate in the gap start to be thermally populated only for temperatures comparable to the Debye frequency, which is much higher than 10 K. The temperature dependence that follows from equation (21) is discussed below.

To simplify formulae, we will look at the temperature dependence of the transition rate in the gap at $\Delta\epsilon \ll \epsilon_c$. The above discussion suggests that there must be such a temperature dependence in order to explain the 300-times decrease of the transition rate in the gap compared to that in bulk at zero temperature. The zero-temperature (spontaneous) value of τ_1^{-1} in this case is $\tau_{1,\mathrm{spont}}^{-1} = 2\kappa\eta$. Next, we assume that $\eta \ll T$ and expand $n_B(\omega_n - i\eta)$ to leading order in η/T:

$$n_B(\omega_n - i\eta) \approx n_B(\omega_n) + i\frac{\eta}{T} n_B(\omega_n)[n_B(\omega_n) + 1]. \tag{26}$$

We substitute the above expansion into (21) and calculate the integral assuming that $\eta, \Delta\epsilon \ll \omega$ in the denominator of the integrand, in accordance with the approximation formulated above (this is a very accurate approximation for $\Delta\epsilon < \omega_{\min}$ and $\eta \sim 10^{-5}$). Then the transition rate is given by

$$\tau_1^{-1} = \tau_{1,\mathrm{spont}}^{-1}\left[1 + 2\left(\frac{T}{\omega_D}\right)^2\left(\int_{\omega_{\min}T}^{\omega_D T}\frac{x\,dx}{\exp(x)-1} + \int_{\omega_{\min}T}^{\omega_D T}\frac{\exp(x)x^2\,dx}{(\exp(x)-1)^2}\right)\right] \tag{27}$$

where $\tau_{1,\mathrm{spont}}^{-1} = 2\kappa\eta$ is the zero-temperature value of the transition rate. The integrals on the right-hand side of (27) have the limiting values of $\pi^2/6$ and $\pi^2/3$ when $T \ll \omega_D$, respectively, and ω_D/T when $T \gg \omega_D$. Therefore, the temperature dependence of τ_1^{-1} in these two limiting cases has the form

$$\tau_1^{-1}(T) = \tau_{1,\mathrm{spont}}^{-1} \times \begin{cases} 1 + \pi^2(T/\omega_D)^2 & \text{if } T \ll \omega_D \\ 1 + 4T/\omega_D & \text{if } T \gg \omega_D. \end{cases} \tag{28}$$

Thus, the induced transition rate is much less than the spontaneous one for $T \ll \omega_D$ and, therefore, the temperature dependence of τ_1^{-1} is not expected to be observable for these temperatures.

4. Broadening of phonons with non-Lorentzian line shapes

In the previous section we saw that the introduction of the damping constant η in the phonon propagator leads to certain unphysical conclusions. This is explained by the fact that the Lorentzian tails decay as $1/\omega^2$ while the weighted DOS grows as ω^3, so an integral of the type (21) does not converge at the upper limit. As is well known [17], this would lead to an

ultraviolet divergence of the transition rate in the case of electromagnetic interaction, when there is no high-frequency cut-off. In the case of phonons, however, the integral stays finite, but the relaxation rate is largely determined by the high-frequency modes.

On the other hand, the absence of temperature dependence for $T \ll \omega_D$ suggests that the transition rate in the gap might indeed be caused by interaction with the high-frequency modes whose occupation numbers stay very small for $T \ll \omega_D$. This makes the relaxation mechanism suggested in the previous section plausible. In this section we suggest how the apparent contradictions discussed above can be removed and the finite transition rate in the gap explained.

First, we note that the energy-independent value of η ensures that phonons decay exponentially over time. The lifetime of a phonon is η^{-1}. However, the exponential time decay can happen even if η is a function of ω, unless we are looking at extremely large times. In fact, this assumption lies at the core of the widely used quasiparticle-pole approximation. Consider the following expression for the (diagonal-in-n) phonon propagator:

$$D_{\mathrm{ret}}(n,\omega) = \frac{1}{\omega - \omega_n - \Pi_{\mathrm{ret}}(n,\omega)}. \tag{29}$$

The function (29) differs from the free propagator (9) by the inclusion of the phonon self-energy $\Pi_{\mathrm{ret}}(n,\omega)$ in the denominator. If one is interested in the phonon relaxation rate, it can be calculated by making the quasiparticle-pole approximation at the phonon's eigenfrequency: $\eta = -\mathrm{Im}\,\Pi_{\mathrm{ret}}(n,\omega=\omega_n)$. The constant η, defined in this way, is experimentally measurable by studying, for example, the energy relaxation of the excited phonons.

However, if we are interested in the electron relaxation rate, the quasiparticle-pole approximation is quite different. By replacing the free propagators in formula (19) by the exact functions $D_{\mathrm{ret}}(n,\omega)$, we obtain for the electron relaxation rate

$$\begin{aligned}\tau_1^{-1} &= -\mathrm{Im}\sum_n g_n^2 \frac{1+n_B(\omega_n)}{\omega - \xi_0 - \omega_n - \Pi_{\mathrm{ret}}(n,\omega-\xi_0)}\bigg|_{\omega=\xi_1} \\ &= -\mathrm{Im}\sum_n g_n^2 \frac{1+n_B(\omega_n)}{\Delta\epsilon - \omega_n - \Pi_{\mathrm{ret}}(n,\Delta\epsilon)}.\end{aligned} \tag{30}$$

As indicated above, we now need to evaluate the phonon self-energy at $\Delta\epsilon$ rather than at ω_n. The results can be quite different from the value of η which is experimentally measured by observing the relaxation of the phonons.

To summarize the arguments outlined above, it is important to retain the frequency dependence of the phonon self-energy $\Pi_{\mathrm{ret}}(n,\omega)$ because it must be evaluated at a frequency which is significantly different from ω_n. The result can be, in fact, much smaller than the experimentally observable relaxation constant $\eta = -\mathrm{Im}\,\Pi_{\mathrm{ret}}(n,\omega_n)$.

In this section we will assume that the phonon self-energy depends on ω and on the quantum number ω_n as

$$\mathrm{Im}\,\Pi_{\mathrm{ret}}(n,\omega) = -\eta\left(\frac{\omega}{\omega_n}\right)^p\left(\frac{\omega_n}{\omega_D}\right)^q. \tag{31}$$

Below we shall show that the form (31) with $p=7$ and $q=8$ applies to phonons broadened by cubic anharmonicity, but for generality we will let p and q be arbitrary at this point. The experimentally measurable phonon relaxation rates for eigenfrequencies close to ω_D are still given by the constant η. However, if we evaluate the right-hand side of the above formula at $\omega = \Delta\epsilon$, the results will be $\sim\eta(\Delta\epsilon/\omega_n)^p$. If $p > 0$ and $\Delta\epsilon \ll \omega_n$, the factor $(\Delta\epsilon/\omega_n)^p$ can become much smaller than unity. Practically, this means that in the case of the Debye DOS without a gap the crossover from the cubic dependence on $\Delta\epsilon$ to a constant at small energies

can be eliminated, and the experimentally observable ratio of the transition rate in the bulk samples and in nanoparticles at $\Delta\epsilon = 3\ \mathrm{cm}^{-1}$ can be explained by a realistic value of η.

Formula (31) reflects the dependence of $\Pi_{\mathrm{ret}}(n, \omega)$ both on ω and n. In the particular case $p = q$, the net result of (31) is to replace η by $\eta(\Delta\epsilon/\omega_{\mathrm{D}})^p$ in the expressions (22)–(25) for the transition rate (at zero temperature). Making this substitution in equation (25), we can easily see that in the case of the Debye DOS without a gap, the crossover from the cubic dependence on $\Delta\epsilon$ to a constant does not take place as long as $\eta \ll 2\omega_{\mathrm{D}}(\omega_{\mathrm{D}}/\Delta\epsilon)^{p-3}$. This inequality always holds if $p \geqslant 3$ and $\eta \ll \omega_{\mathrm{D}}$. The last statement is experimentally known to be true.

It is easy to generalize for arbitrary $p \neq q$. For simplicity, we show the result for $T \ll \omega_{\min}$ when the Bose occupation numbers $n_{\mathrm{B}}(\omega_n)$ are all small compared to unity and can be neglected. We also assume that $\omega_{\min} \ll \omega_{\mathrm{D}}$ and obtain

$$\tau_1^{-1} = 4\kappa\eta\left(\frac{\Delta\epsilon}{\omega_{\mathrm{D}}}\right)^p \int_0^1 \frac{x^{3+q-p}\,\mathrm{d}x}{(\Delta\epsilon/\omega_{\mathrm{D}} - x)^2 + (\eta/\omega_{\mathrm{D}})^2(\Delta\epsilon/\omega_{\mathrm{D}})^{2p}x^{2(p-q)}}. \tag{32}$$

(In the lower integration limit, we have replaced $\omega_{\min}/\omega_{\mathrm{D}}$ by 0.) For $\Delta\epsilon$ in the gap and positive p, we have $\Delta\epsilon/\omega_{\mathrm{D}}$, $(\eta/\omega_{\mathrm{D}})^2(\Delta\epsilon/\omega_{\mathrm{D}})^{2p} \ll 1$, and the above integral can be approximated as

$$\tau_1^{-1} = 4\kappa\eta\left(\frac{\Delta\epsilon}{\omega_{\mathrm{D}}}\right)^p \int_0^1 x^{1+q-p}\,\mathrm{d}x. \tag{33}$$

In accordance with the observed absence of the temperature dependence of the transition rate, we require that the latter be determined mainly by the inputs of high-frequency modes. Mathematically, this means that the above integral must converge at the lower limit, or $2 + q - p > 0$. Then

$$\tau_1^{-1} = \frac{4\kappa\eta}{2+q-p}\left(\frac{\Delta\epsilon}{\omega_{\mathrm{D}}}\right)^p. \tag{34}$$

Analogously to the case $p = q$, we search for the condition when there is no crossover from cubic dependence of $\Delta\epsilon$ to a constant at small energies in the case of a Debye DOS without a gap. This condition is that the input of high-frequency modes given by (34) is much smaller than the first term on the right-hand side of (25), $4\pi\kappa(\Delta\epsilon)^3/\omega_{\mathrm{D}}^2$. This translates to $\eta \ll (2 + q - p)\omega_{\mathrm{D}}(\omega_{\mathrm{D}}/\Delta\epsilon)^{p-3}$. Again, this inequality holds for $p \geqslant 3$.

So far, we have formulated two requirements for constants p and q: $p \geqslant 3$ and $q > p - 2$. The first inequality guarantees that the dependence of the transition rate on the energy level separation is cubic for bulk samples, in accordance with experimental data. The second condition guarantees that the transition rate for the energy level separation below the gap in a nanoparticle is governed by the tails of high-frequency modes and is, therefore, insensitive to temperature as long as the latter is much less than the Debye temperature. In the next section we calculate $\mathrm{Im}\,\Pi_{\mathrm{ret}}(n, \omega)$ for the case of phonon interaction due to cubic anharmonicity and show that it has the same form as (31) with p and q satisfying the above conditions in the case of the Debye DOS without a gap. Unfortunately, the cubic anharmonicity alone cannot quantitatively explain the experimentally observed electron decay rates.

5. Relaxation of phonons due to cubic anharmonicity

Cubic anharmonicity of the lattice can be described by the interaction Hamiltonian [13]

$$\delta H_{\mathrm{ph}} = K\Phi^3 \tag{35}$$

where

$$\Phi \equiv \sum_n g_n(a_n + a_n^\dagger) \tag{36}$$

is the (scalar) strain field. For simplicity we will ignore the actual tensor structure of the phonons and their anharmonic interaction, as these do not affect the results qualitatively. We calculate the phonon Green's function using the perturbation theory. In the leading (second) order there are two distinct diagrams (taking into account the time direction of the phonon propagators) to be evaluated:

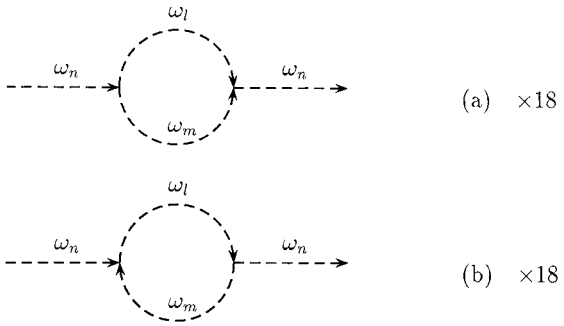

where the multiplicity of each diagram has also been indicated. Diagram (a) describes the second-harmonic generation and can occur at zero temperature. Diagram (b) describes combination scattering which requires the existence of a thermal phonon (ω_m).

The contributions of the diagrams (a) and (b) to the phonon self-energy are

$$-\mathrm{Im}\,\Pi^{(a)}_{\mathrm{ret}}(n,\omega) = 9\pi K^2 g_n^2 \int \Gamma(\omega-\omega')\Gamma(\omega')[1+n_{\mathrm{B}}(\omega')+n_{\mathrm{B}}(\omega-\omega')]\,\mathrm{d}\omega' \tag{37}$$

$$-\mathrm{Im}\,\Pi^{(b)}_{\mathrm{ret}}(n,\omega) = 9\pi K^2 g_n^2 \int \Gamma(\omega'-\omega)\Gamma(\omega')[n_{\mathrm{B}}(\omega'-\omega)-n_{\mathrm{B}}(\omega')]\,\mathrm{d}\omega'. \tag{38}$$

We start by analysing the above results at zero temperature. In this case, the only non-zero term comes from the second-harmonic generation (37):

$$-\mathrm{Im}\,\Pi_{\mathrm{ret}}(n,\omega) = 9\pi K^2 g_n^2 \int \Gamma(\omega-\omega')\Gamma(\omega')\,\mathrm{d}\omega' \qquad (T=0). \tag{39}$$

In the case of a Debye DOS without a gap, the above integral is equal to

$$-\mathrm{Im}\,\Pi_{\mathrm{ret}}(n,\omega) = \frac{9\pi K^2}{140}\left(\frac{4\kappa}{\omega_{\mathrm{D}}^2}\right)^2 g_n^2\omega^7 \qquad (T=0,\omega_{\min}=0). \tag{40}$$

We see that the phonon self-energy has the functional form (31) with $p=7$ and $q=8$. Both constants satisfy the inequalities formulated in the previous section. Therefore, the broadening of phonons due to cubic anharmonicity does not lead to unphysical results in the case of the bulk DOS. Note that the $\propto\omega^7$ dependence was obtained because the interaction considered in this section does not conserve momentum. If we require momentum conservation (e.g., in bulk samples), the result will be similar with $p=5, q=6$, also satisfying the inequalities formulated above.

In the case of $\omega_{\min} > 0$, equation (39) does not lead to the functional form (31). In particular, it is easy to see that $\mathrm{Im}\,\Pi_{\mathrm{ret}}(n,\omega)=0$ if $\omega<\omega_{\min}$. Cubic anharmonicity alone is not sufficient to explain the electronic transitions in the gap at zero temperature. Physically, this fact can be easily understood. Since the Hamiltonian (35) does not involve interaction with the outside environment, the broadened DOS is non-zero only for frequencies that can be constructed as combinations of the type $\omega=\omega_n+\omega_{n'}$ (combination frequencies) where ω_n and $\omega_{n'}$ are two frequencies of the free vibrational modes. Since there are no eigenfrequencies below the acoustic gap, there are no combination frequencies there either.

Now we turn to the finite-temperature term that follows from diagram (b). To relate the anharmonic coupling constant K to experimentally measurable quantities, we introduce

the zero-temperature phonon decay rate for vibrational modes close to the Debye frequency, η_D. For temperatures much smaller than the Debye one, this rate comes predominantly from second-harmonic generation (diagram (a)) and, therefore, $\eta_D = -\mathrm{Im}\,\Pi^{(a)}_{\mathrm{ret}}(N, \omega_N)$, where N (the total number of vibrational modes) labels the mode with the highest available frequency (ω_D). According to (40),

$$\eta_D = \frac{9\pi K^2}{140}\left(\frac{4\kappa}{\omega_D^2}\right)^2 g_N^2 \omega_D^7. \tag{41}$$

Taking into account that $g_n^2 = g_N^2 \omega_n/\omega_D$, we can rewrite (38) as

$$-\mathrm{Im}\,\Pi^{(b)}_{\mathrm{ret}}(n, \omega) = \eta_D \frac{\omega_n}{\omega_D}\, I\left(\frac{\Delta\epsilon}{\omega_D}, \frac{T}{\omega_D}, \frac{\omega_{\min}}{\omega_D}\right) \tag{42}$$

where

$$I(x, y, z) \equiv 140 \int_z^1 \xi^3 (\xi - x)^3 \left[\frac{1}{\exp(\{\xi - x\}/y) - 1} - \frac{1}{\exp(\xi/y) - 1}\right] \mathrm{d}\xi. \tag{43}$$

The behaviour of the integral I as a function of relative temperature T/ω_D for several sets of parameters is illustrated in figure 2.

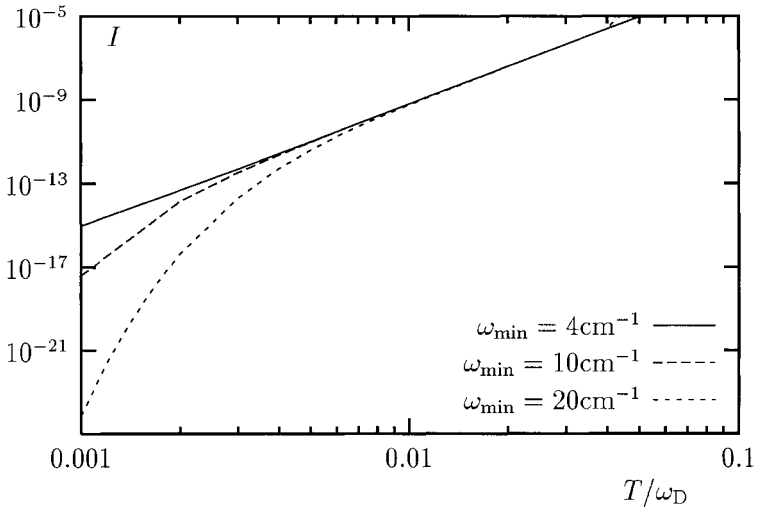

Figure 2. Integral $I(\Delta\epsilon/\omega_D, T/\omega_D, \omega_{\min}/\omega_D)$ as a function of T/ω_D for $\omega_D = 500\ \mathrm{cm}^{-1}$, $\Delta\epsilon = 3\ \mathrm{cm}^{-1}$, and for different values of $\omega_{\min}$.

As follows from (30), the electron transition rate is given by

$$\tau_1^{-1} = \int_{\omega_{\min}}^{\omega_D} \Gamma(\omega')\left[1 + n_B(\omega')\right] \frac{-\mathrm{Im}\,\Pi^{(b)}_{\mathrm{ret}}(\omega', \Delta\epsilon)}{(\Delta\epsilon - \omega')^2 + [\mathrm{Im}\,\Pi^{(b)}_{\mathrm{ret}}(\omega', \Delta\epsilon)]^2}\, \mathrm{d}\omega' \tag{44}$$

where we have substituted for the formal argument of the phonon self-energy functional dependence on n with the corresponding frequency ω_n; integration in (44) is over this argument.

Since we are interested in the electronic transition rate in the gap at small temperatures, we make the following approximations, which are essentially analogous to the ones outlined in the previous section. We neglect the factor $\Pi^{(b)}$ in the denominator of (44), assume that

$(\Delta\epsilon - \omega')^2 \approx (\omega')^2$, neglect the Bose occupation factor n_B, and extend integration from 0 to ω_D, which results in

$$\tau_1^{-1} = \frac{4\kappa}{3} I\left(\frac{\Delta\epsilon}{\omega_D}, \frac{T}{\omega_D}, \frac{\omega_{min}}{\omega_D}\right)\eta_D. \tag{45}$$

Taking into account that the transition rate at the same energy in the bulk is given by $4\pi\kappa\Delta\epsilon^3/\omega_D^2$, we can estimate the ratio of the transition rates in nanoparticles with the acoustic gap to that in large samples as

$$\frac{\tau_1^{-1}[\text{gap}]}{\tau_1^{-1}[\text{bulk}]} = \frac{I(\Delta\epsilon/\omega_D, T/\omega_D, \omega_{min}/\omega_D)}{3\pi}\frac{\eta_D\omega_D^2}{\Delta\epsilon^3}. \tag{46}$$

The integral I is plotted in figure 2 as a function of T/ω_D for $\Delta\epsilon = 3\ \text{cm}^{-1}$, $\omega_D = 500\ \text{cm}^{-1}$, and several values of ω_{min}. As can be seen from the figure, I is described by a power-law function of T/ω_D for large temperatures and is exponentially small for $T \ll \omega_D$. The characteristic value of T/ω_D for which the crossover from the power to exponential behaviour takes place decreases as ω_{min} approaches $\Delta\epsilon$. The numerical values of the integral are extremely small for realistic values of the parameters and temperatures of the order of ω_{min}. For example, for $\Delta\epsilon = T = 4\ \text{cm}^{-1}$ and $\omega_{min} = 4\ \text{cm}^{-1}$, $I \approx 2.9 \times 10^{-11}$. By using (46) with the known ratio $\tau_1^{-1}[\text{gap}]/\tau_1^{-1}[\text{bulk}] \approx 1/300$ and the above value of I, we arrive at the conclusion that η_D must be as large as $\approx 1.2 \times 10^7\ \text{cm}^{-1}$ in order to be consistent with experimental results.

6. Summary and discussion

We have calculated the frequency and temperature dependence of the one-phonon relaxation rate for an electronic transition below the acoustic gap in nanocrystals that is made possible due to anharmonic broadening of phonon modes. Although the cubic anharmonicity provides a finite-temperature mechanism for the direct one-phonon process, it is insufficient for explaining experimental rates that were observed at low temperatures. The physical reason for this is that anharmonicity alone does not provide any mechanism for energy dissipation from the nanoparticle. Such dissipation is required by energy conservation, because the energy of the initial and final states must be the same, but the electronic energy cannot be absorbed by phonons at zero temperature because all the phonon modes are above the acoustic gap. At finite temperature, the electronic transition energy can be accommodated by absorbing a thermal phonon and then emitting a phonon of higher frequency. This process leads to a state with the same energy as the initial one.

We conclude that in order to describe electronic transitions in the acoustic gap at low temperatures, the interaction Hamiltonian should contain terms that allow energy exchange with the surroundings. Accordingly, no such transitions should be possible in truly isolated nanoparticles. The latter prediction can be verified experimentally by comparing the transition rates in systems of aggregated and non-aggregated nanocrystals.

Acknowledgments

This work was supported by a Faculty Research Grant awarded by the University of Georgia Research Foundation and by a Research Innovation Award from the Research Corporation. It is a pleasure to thank William Dennis, Richard Meltzer and Ho-Soon Yang for useful discussions.

References

[1] Ashcroft N W and Mermin N D 1976 *Solid State Physics* (Philadelphia, PA: Saunders)
[2] Henderson B and Imbusch G F 1989 *Optical Spectroscopy of Inorganic Solids* (Oxford: Clarendon)
[3] Kuzmany H 1998 *Solid-State Spectroscopy: an Introduction* (Berlin: Springer)
[4] Collins R W *et al* (ed) 1995 *Microcrystalline and Nanocrystalline Semiconductors (Mater. Res. Soc. Symp. Proc. No 358)* (Pittsburgh, PA: Materials Research Society)
[5] Gaponenko S V 1998 *Optical Properties of Semiconductor Nanocrystals* (Cambridge: Cambridge University Press)
[6] Leburton J P *et al* (ed) 1993 *Phonons in Semiconductor Nanostructures* (Dordrecht: Kluwer–Academic)
[7] Woggon U 1997 *Optical Properties of Semiconductor Quantum Dots* (Berlin: Springer)
[8] Jacak L, Hawrylak P and Wójs A 1998 *Quantum Dots* (Berlin: Springer)
[9] Bockelmann U and Bastard G 1990 *Phys. Rev.* B **42** 8947
[10] Woggon U, Gaponenko S V, Uhrig A, Langbein W and Klingshirn C 1994 *Adv. Mater. Opt. Electron.* **3** 141
[11] Yang H S, Feofilov S P, Williams D K, Milora J C, Tissue B M, Meltzer R S and Dennis W M 1999 *Physica* B **263** 476
[12] Yang H S, Hong K S, Feofilov S P, Tissue B M, Meltzer R S and Dennis W M 1999 *J. Lumin.* **83** 139
[13] Mahan G D 1990 *Many-Particle Physics* (New York: Plenum)
[14] Scully M O and Zubairy M S 1997 *Quantum Optics* (Cambridge: Cambridge University Press)
[15] This definition differs from the definition adopted in most standard texts (e.g., see [13]), where phonon propagators have no time direction.
[16] Meltzer R S and Rives J E 1977 *Phys. Rev.* B **15** 2442
[17] Pippard A B 1983 *The Physics of Vibrations. The Simple Vibrator in Quantum Mechanics* vol 2 (Cambridge: Cambridge University Press)